ChemPubSoc Europe

DOI: 10.1002/chem.201504214

CHEMISTRY A European Journal Full Paper

Porphyrinoids |*Hot Paper*|

2*H*-Tetrakis(3,5-di-*tert*-butyl)phenylporphyrin on a Cu(110) Surface: Room-Temperature Self-Metalation and Surface-Reconstruction-Facilitated Self-Assembly

Liang Zhang,[a, b] Michael Lepper,[a, b] Michael Stark,[a, b] Ralf Schuster,[a, b] Dominik Lungerich,[b, c] Norbert Jux,[b, c] Hans-Peter Steinrück,[a, b] and Hubertus Marbach*[a, b]

Abstract: The adsorption behavior of 2*H*-tetrakis(3,5-di-*tert*-butyl)phenylporphyrin (2HTTBPP) on Cu(110) and Cu(110)–(2×1)O surfaces have been investigated by using variable-temperature scanning tunneling microscopy (STM) under ultrahigh vacuum conditions. On the bare Cu(110) surface, individual 2HTTBPP molecules are observed. These molecules are immobilized on the surface with a particular orientation with respect to the crystallographic directions of the Cu(110) surface and do not form supramolecular aggregates up to full monolayer coverage. In contrast, a chiral supramolecular structure is formed on the Cu(110)–(2×1)O surface, which is stabilized by van der Waals interactions between the *tert*-butyl groups of neighboring molecules. These findings are explained by weakened molecule–substrate interactions on the Cu(110)–(2×1)O surface relative to the bare Cu(110) surface. By comparison with the corresponding results of Cu–tetrakis(3,5-di-*tert*-butyl)phenylporphyrin (CuTTBPP) on Cu(110) and Cu(110)–(2×1)O surfaces, we find that the 2HTTBPP molecules can self-metalate on both surfaces with copper atoms from the substrate at room temperature (RT). The possible origins of the self-metalation reaction at RT are discussed. Finally, peculiar irreversible temperature-dependent switching of the intramolecular conformations of the investigated molecules on the Cu(110) surface was observed and interpreted.

Introduction

The investigation of ordered organic nanoarchitectures on well-defined surfaces is mainly driven by two goals.[1–9] The first goal is to improve the efficiency of organic electronic devices, such as organic light-emitting diodes, field-effect transistors, and photovoltaic devices. The second more fundamental motivation is to gain insight into the adsorption behavior of organic molecules and, in particular, to investigate the specific contributions of molecule–substrate and molecule–molecule interactions. This knowledge might be used in the next step to extract design rules for the controlled fabrication of nanostructures from organic molecules.

Porphyrins are particularly well suited as molecular building blocks for the generation of functional molecular devices because they combine an intrinsic functionality, which is mainly determined by the central metal atom, with a rigid structural theme, which often triggers long-range order on surfaces.[3,5,6,8–10] In this context, scanning tunneling microscopy (STM) has proven to be a powerful tool to investigate the supramolecular arrangement, intramolecular conformation, and electronic structure of large organic molecules on solid surfaces.[1,2,5,11] For example, extensive STM investigations have been performed for porphyrins on different surfaces, thus demonstrating that their adsorption behavior, such as intramolecular conformation and supramolecular arrangement, is strongly dependent on the actual substrate,[12,13] adsorbate coverage,[14] and the functional side groups attached to the porphyrin marcocycle.[12,15–17]

Generally, the adsorption behavior of porphyrins is determined by a subtle balance between molecule–molecule and molecule–substrate interactions. For example, for 2*H*-tetraphenylporphyrin (2HTPP) on a Cu(111) surface, the strong chemical interaction between the iminic nitrogen atoms of the porphyrin and copper substrate atoms leads to a strong change in intramolecular conformation and pronounced site specificity; consequently, individual molecules can be observed, even at room temperature, due to the resulting low mobility.[16,18,19] In contrast, on Ag(111) surfaces no specific molecule–substrate interactions exist; therefore, supramolecular arrangements of

[a] *Dr. L. Zhang, M. Lepper, M. Stark, R. Schuster, Prof. Dr. H.-P. Steinrück, Dr. H. Marbach*
Lehrstuhl für Physikalische Chemie II, Universität Erlangen-Nürnberg
Egerlandstrasse 3, 91058 Erlangen (Germany)
E-mail: hubertus.marbach@fau.de

[b] *Dr. L. Zhang, M. Lepper, M. Stark, R. Schuster, D. Lungerich, Prof. Dr. N. Jux, Prof. Dr. H.-P. Steinrück, Dr. H. Marbach*
Interdisciplinary Center for Molecular Materials (ICMM)
Universität Erlangen-Nürnberg (Germany)

[c] *D. Lungerich, Prof. Dr. N. Jux*
Lehrstuhl für Organische Chemie II, Universität Erlangen-Nürnberg
Henkestrasse 42, 91054 Erlangen (Germany)

Supporting information for this article is available on the WWW under http://dx.doi.org/10.1002/chem.201504214.

2HTPP are formed caused by the T-type intermolecular interactions between the peripheral phenyl substituents of neighboring molecules.[20]

So far, most studies have focused on the adsorption of porphyrins on bare substrates. Only a few investigations have compared the different adsorption behaviors of porphyrins on bare and adsorbate-induced reconstructed surfaces.[21–23] In general, such a surface reconstruction can decrease the surface reactivity and result in the formation of supramolecular structures, whereas the corresponding bare surface only causes disordered molecular structures (e.g., terephthalic acid (TPA) and 2,3,2′,3′-(tetrabromophenyl-6,6′)biquinoxalinyl (TBPBQ) on Si(111)–($\sqrt{3}\times\sqrt{3}$)Ag[24] and Cu(110)–(2×1)O[25] surfaces, respectively). In contrast, a surface reconstruction may also increase the surface reactivity, for example, as observed for the self-metalation of 2HTPP on Cu(001)–($2\sqrt{2}\times\sqrt{2}$)*R*45°-O.[22] Therefore, surface reconstructions can be regarded as a suitable route to tailor molecular architectures by using a bottom-up approach.[26–28]

Generally the {110} facet of face-centered cubic (fcc) metals exhibits an intrinsic anisotropy due to the close-packed metal rows along the [1$\bar{1}$0] direction. This unidirectional surface corrugation makes the substrate especially appealing for the preparation of a one-dimensional (1D) assembly of organic molecules.[25,27–30] This property and the "open structure" of corresponding (110) surfaces usually makes these substrates more reactive. An illustrative example is the recently reported self-metalation of the free-base phthalocyanine (2HPc) with silver atoms from a Ag(110) substrate, which does not occur on the corresponding Ag(111) surface.[29] The Cu(110) surface is another frequently used substrate for the self-assembly of organic molecules.[25–27] In addition, the Cu(110)–(2×1)O surface reconstruction has an even more pronounced corrugation, with the close-packed Cu–O rows orientated along the [001] direction.[31,32] Moreover, the reconstructed surface exhibits a modified reactivity relative to a bare Cu(110) surface due to the different structure and the presence of oxygen atoms.[33]

Herein, we use STM to investigate the growth of 2*H*-tetrakis(3,5-di-*tert*-butyl)phenylporphyrin (2HTTBPP; Figure 1) on Cu(110) and Cu(110)–(2×1)O surfaces and compare the results to the corresponding metalloporphyrin, namely, Cu–tetrakis(3,5-di-*tert*-butyl)phenylporphyrin (CuTTBPP), on the same surfaces. We show that the reconstruction of the Cu(110) surface by oxygen atoms facilitates the self-assembly of a supramolecular structure of 2HTTBPP molecules by decreasing molecule–substrate interactions. In addition, we prove that the so-called self-metalation reaction of 2HTTBPP (to yield CuTTBPP) occurs on both surfaces at room temperature (RT).

Results and Discussion

After the deposition of 2HTTBPP onto a Cu(110) surface at 180 K, a large-area STM image measured at 200 K shows a statistical distribution of the adsorbed molecules on the surface without a preference for certain sites, such as the step edges (Figure 2a). In addition, time sequences of the STM images reveal that the 2HTTBPP molecules are immobile on the surface, that is, no diffusion or indications of rotational events are observed. This observation is attributed to a strong site-specific molecule–substrate interaction combined with the decreased surface temperature.[6,18,34] In contrast, 2HTTBPP molecules on the Cu(111) surface are not static, but rotate around the surface normal at 200 K, even though assembled in a supramolecular order.[6] Therefore, we suggest that the suppressed diffusion and rotation of 2HTTBPP on the Cu(110) surface at 200 K is mainly caused by an even stronger interaction between the molecules and the substrate.

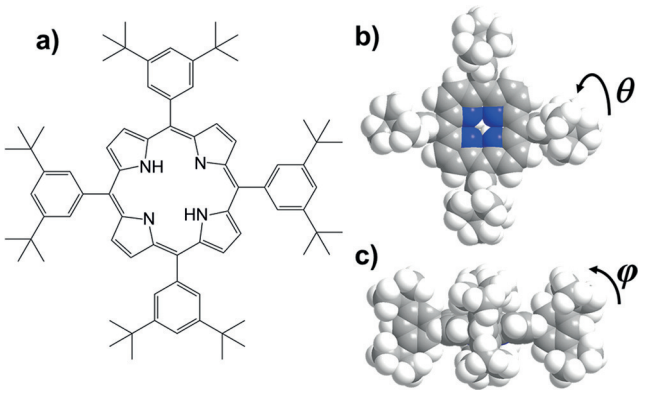

Figure 1. a) Chemical structure of 2HTTBPP. b,c) Top and side views of a DFT gas-phase-optimized space-filling model of 2HTTBPP, respectively.[36,37] The conformation of 2HTTBPP is characterized as the twist and tilt angles of the tBP substituents: θ describes the twist angle of the tBP groups around the macrocycle–phenyl bond and φ represents the tilt angle of the tBP groups out of the macrocycle plane.

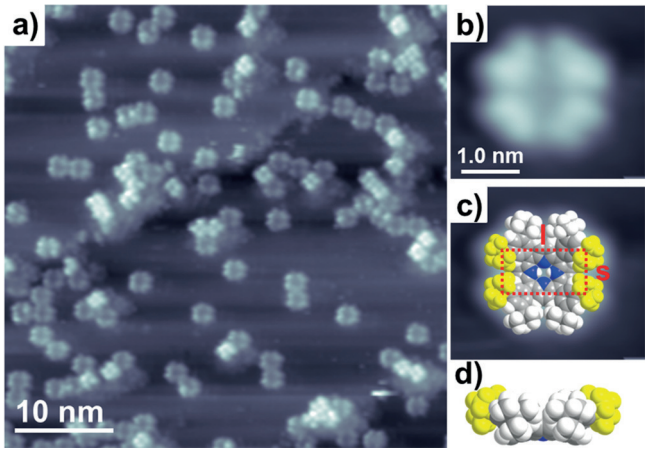

Figure 2. a) Constant-current STM image measured at 200 K after the deposition of 2HTTBPP on a Cu(110) surface at 180 K. b) Molecularly resolved image of a single 2HTTBPP molecule. c) Micrograph from (b) superimposed with a correspondingly scaled molecular model. d) Side view of the molecular model, in which the four upper *tert*-butyl groups are depicted in yellow. Tunneling parameters: $U=-1.1$ V, $I=30$ pA.

Figure 2b shows a high-resolution STM image of a single 2HTTBPP molecule on the Cu(110) surface that exhibits four paired lobes, in which there is a brighter/larger and darker/smaller lobe in each pair. It is well established that the appearance of individual di-*tert*-butyl-phenylporphyrin (TTBPP) molecules in STM images is dominated by the four upper *tert*-butyl

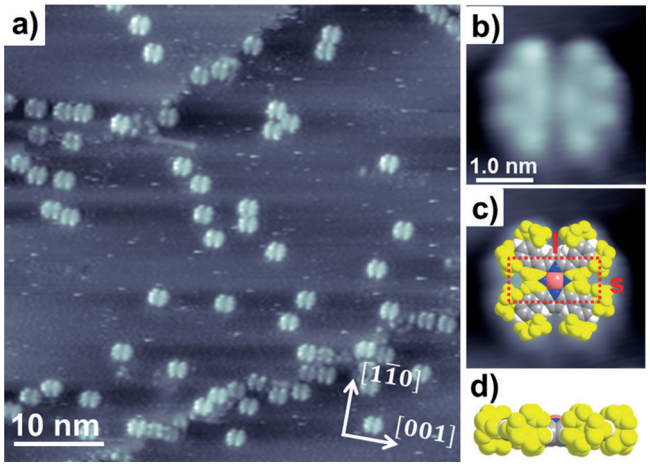

Figure 3. a) Constant-current STM image of 2HTTBPP on a Cu(110) surface with deposition and measurement temperatures at RT. The 2HTTBPP molecules react with the substrate copper atoms and form CuTTBPP molecules at RT. b) Magnified and rotated details of a single CuTTBPP molecule. c) The micrograph from (b) superimposed with a scaled molecular model. d) Side view of the molecular model, in which the eight *tert*-butyl groups and the two upward bent pyrrole rings are depicted in yellow. Tunneling parameters: $U=-1.3$ V, $I=30$ pA.

groups, which form a rectangle in the STM image.[6,12,34,35] The side lengths *l* and *s* of the rectangle are indicated in Figure 2c (and later also in Figures 3c and 6d,h). From this rectangle, the intramolecular conformation (i.e., twist θ and tilt φ angles of the di-*tert*-butylphenyl (tBP) substituents; c.f. Figure 1) can be extracted from the perimeter and aspect ratio (a sketch to illustrate this procedure and additional information are provided in the Supporting Information).[6,16,34] Various intramolecular conformations of the TTBPP species on different substrates have been reported that were derived by using this approach, such as $\theta=40$, $\varphi=6^\circ$ for CuTTBPP on Ag (110),[36] $\theta=75$, $\varphi=5^\circ$ for CuTTBPP on Cu(111),[34] and $\theta=5$, $\varphi=35^\circ$ for 2HTTBPP on Cu(111).[6,34]

For 2HTTBPP on a Cu(110) surface, the extracted values of $l=1.32\pm0.05$ and $s=0.69\pm0.05$ nm yield an intramolecular conformation with $\theta=10\pm5$ and $\varphi=30\pm5^\circ$ (see Figure 2c,d and the Supporting Information for details). This intramolecular conformation is quite different from the one expected for the isolated molecule in the gas phase ($\theta=70$ and $\varphi=0^\circ$),[37] but similar to the conformation of the same molecule on a Cu(111) surface arranged in a peculiar supramolecular order ($\theta=5\pm5$ and $\varphi=35\pm5^\circ$).[6,34] The actual intramolecular conformation is therefore attributed to a "deformation" due to attractive molecule–substrate interactions with a strong site specificity.[30,34,38] Notably, a local minimum was located at very similar twist and tilt angles ($\theta=10$ and $\varphi=30^\circ$), albeit at a relatively high total energy, as reported in a recent density functional theory (DFT) study of the energy surface of the very similar Co–TTBPP molecule in the gas phase.[37]

In addition to the just described molecules with four paired lobes, a minor fraction of molecules with a different appearance (i.e., four protrusions), can been seen in Figure 2a; thus, a different conformation is observed. These molecules are most likely "surface-decoupled" 2HTTBPP molecules on top of molecules in direct contact with the substrate.

The low-temperature (LT) intramolecular conformation observed in Figure 2b at 200 K is thermally unstable, but irreversibly transforms into a different conformation after warming to RT (see Figure S2 in the Supporting Information). The identical conformation can also be achieved by directly depositing 2HTTBPP on a Cu(110) surface at RT (Figure 3a). Similar to the behavior at 200 K, the molecules do not form extended self-assembled domains, even at coverages close to one monolayer at RT. The molecules are again randomly distributed over the surface, thus indicating that the strong site specificity of the molecule–substrate interaction is preserved. The STM images show that each molecule appears as eight equally bright protrusions organized into two quadruplets that surround two oblong protrusions in the center (Figure 3b). By considering the molecular dimensions, we assigned each surrounding protrusion to one *tert*-butyl group and the two central protrusions to the upward bent pyrrole rings due to intramolecular steric repulsions with the adjacent tBP groups.

From the dimensions of the rectangle formed by the four protrusions in the STM image in Figure 3b,c, we derived side lengths of $l=1.41\pm0.05$ and $s=0.76\pm0.05$ nm, which correspond to a conformation with the angles $\theta=0$ and $\varphi=0^\circ$. A schematic drawing of this conformation is shown in Figure 3c,d; please note that the conformational change between 200 and 300 K accompanies the metalation of 2HTTBPP to CuTTBPP by the substrate atoms (see the discussion below). Interestingly, the molecules in the RT and LT phases have the same azimuthal orientation relative to the Cu(110) substrate, despite the fact that their intramolecular conformations are significantly different (c.f. Figures 2 and 3a).

Principally, there are three possibilities that might cause the intramolecular conformation change from the LT to the RT phase: 1) dehydrogenation of 2HTTBPP with the formation of new intramolecular C–C bonds;[39–41] 2) an activated transition toward a more stable conformation of 2HTTBPP at higher temperature;[30,36] and 3) the already mentioned self-metalation of 2HTTBPP by substrate atoms.[10,34,40,42] For porphyrins on metal surfaces, dehydrogenation at RT has rarely been reported. Moreover, the pyrrole groups of the macrocrocycle should fuse with the phenyl rings and become parallel to the Cu(110) surface if dehydrogenation occurs at RT, which certainly is not the case here.[40,41,43] Therefore, we rate the dehydrogenation of 2HTTBPP on the Cu(110) surface at RT as highly unlikely, but instead consider both the activated transition and metalation as sources of the conformational change.

To gain additional insight, we also investigated the adsorption behavior of the metalated version, that is, CuTTBPP on Cu(110) at 200 K (Figure 4). In contrast to the examples discussed above, individual CuTTBPP molecules at 200 K only exhibit four protrusions arranged in a square with a comparably small perimeter. The corresponding analysis yields a conformation with angles of $\theta=90$ and $\varphi=45^\circ$. The small number of dim molecules with different intramolecular conformations under the given measurement conditions probably originate from 2HTTBPP molecules, which are most likely already present

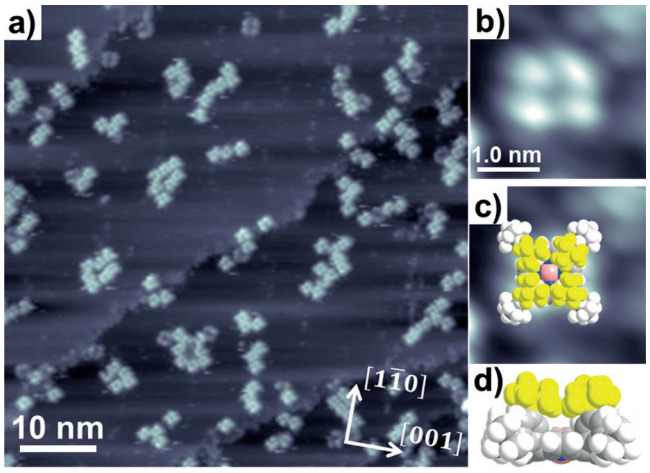

Figure 4. a) Constant-current STM image measured at 200 K after the deposition of CuTTBPP on a Cu(110) surface at 180 K. b) Magnified and rotated details of a single CuTTBPP molecule. c) The micrograph from (b) superimposed with a correspondingly scaled molecular model. d) Side view of the molecular model, in which the four upper *tert*-butyl groups are depicted in yellow. Tunneling parameters: $U=-1.0$ V, $I=29$ pA.

in the CuTTBPP material before evaporation onto the substrate.[44] A summary of the intramolecular conformations with the corresponding errors is given in Table S1 in the Supporting Information. Interestingly, despite their very different intramolecular conformations at 200 K, 2HTTBPP and CuTTBPP transform into the same conformation at RT (c.f. Figure 5). In other words, although 2HTTBPP and CuTTBPP have different initial states at 200 K, these molecules reach the same final state at RT. These observations are a strong indication that 2HTTBPP molecules self-metalate with copper substrate atoms to form CuTTBPP molecules at RT and this process goes along with a change of the intramolecular conformation (Figure 3 c, d).[19,34,40,45] Moreover, the intramolecular conformation does not change after heating the sample in Figure 3 to 450 K, which is the highest temperature reported so far for the self-metalation of porphyrins with copper substrate atoms,[7,19,34,42,46,47] thus further corroborating the proposed self-metalation of 2HTTBPP at RT. Notably, the possibility to self-metalate free-base porphyrin molecules at RT on Cu(110) surfaces has been reported previously for protoporphyrin IX.[47,48]

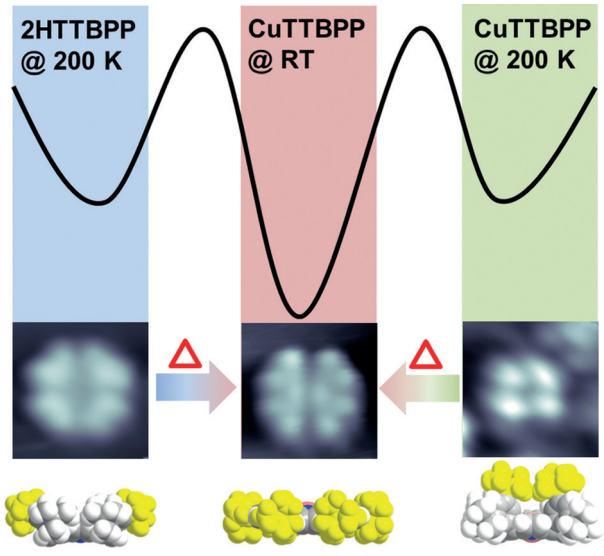

Figure 5. Schematic illustration of the energy scheme for 2HTTBPP and CuTTBPP on Cu(110) surfaces at the indicated temperatures. Note that the 2HTTBPP molecules react with the substrate copper atoms and form CuTTBPP molecules at RT. The bottom shows the molecularly resolved STM image of single molecule and a side view of the corresponding molecular model. Tunneling parameters: $U=-1.1$ V, $I=30$ pA (left); $U=-1.3$ V, $I=30$ pA (middle); and $U=-1.0$ V, $I=29$ pA (right).

Interestingly, the intramolecular conformation of CuTTBPP also changes irreversibly from 200 K to RT (see Figure 5 and Figure S3 in the Supporting Information). This finding is especially remarkable because the conformational change is much more pronounced than for 2HTTBPP, even though the latter undergoes a chemical transformation, namely, the self-metalation reaction to CuTTBPP. Although 2HTTBPP and CuTTBPP exhibit a "flat" conformation at 200 K and RT, respectively, with the macrocycle close to the surface, CuTTBPP is in a conformation at 200 K in which the macrocycle is rather elevated from the substrate.

This observation can be explained as follows: The overall energetically most favorable situation is with CuTTBPP at RT. We propose that the specific flat conformation of this species, with the whole molecule very close to the surface, is driven by attractive van der Waals interactions with the substrate, which are strongest for this arrangement. In the somewhat similar conformation of 2HTTBPP at 200 K, the center of the molecule is close to the surface, whereas the periphery is farther away, thus resembling a bowl shape.[6] This geometry is in line with a domination of the strong attractive interaction of the iminic nitrogen atoms in the macrocycle and the copper substrate, which was reported for different free-base porphyrins on copper surfaces.[14,18,40,42] The absence of a central protrusion also indicates that all four pyrrol groups of 2HTTBPP are bent toward the surface, whereas the peripheral substituents are bent in the opposite direction. This orientation can be explained by a strong steric hindrance of the rotation of the *ortho* substituents, which cannot be overcome at 200 K. The conformation of CuTTBPP at 200 K also resembles a situation in which the macrocycle is close to the surface, whereas the peripheral substituents are strongly tilted away from the surface. Even though the situation appears similar to 2HTTBPP at 200 K at first glance, we propose that the saddle-shaped conformation for CuTTBPP is preserved due to a higher tensile stress in the macrocycle due to the complexed central metal copper atom.[20] However, similar to the situation described for 2HTTBPP at 200 K, we propose that the strong steric hindrance of the *ortho*-substituent rotation cannot be overcome for CuTTBPP at 200 K either. Consequently the transition to the energetically favorable flat intramolecular conformation is a result of the additional thermal energy at RT, which is sufficient to overcome the corresponding steric repulsion (c.f. Figure 5).

In a previous study on a Cu(111) surface, we demonstrated that full self-metalation of a 2HTTBPP layer occurs after annealing the sample to 450 K for 2 minutes,[34] that is, at a higher

temperature than the self-metalation on a Cu(110) surface at RT reported herein. We propose that the self-metalation at lower temperatures observed in our present study is correlated to the much higher number of copper adatoms (by a factor of 10^4) on a Cu(110) surface relative to a Cu(111) surface at RT,[49] which should facilitate self-metalation of 2HTTBPP to CuTTBPP.[19,42,48] The importance of metal adatoms was recently indicated by Goldoni et al. based on DFT calculations for the metalation of 2HTPP on a Ni(111) surface.[46] One interesting aspect to be noted here is the low mobility of CuTTBPP at RT. Although common for metal-free porphyrins on copper substrates,[5,7,18,22] this low mobility has not been observed for metalated porphyrins on other copper surfaces.[6,13,50,51] We tentatively propose that the *tert*-butyl groups in the molecule are in a specific registry with the Cu(110) surface, thus hindering diffusion and rotation on the surface at RT.[52,53]

Based on the discussions above, we conclude that the 2HTTBPP and CuTTBPP (after metalation) molecules do not form supramolecular structures on a Cu(110) surface due to strong site-specific molecule–substrate interactions. To evaluate the role of the surface further, we also investigated the adsorption behavior of 2HTTBPP on the (2×1)O-reconstructed Cu(110) surface. A typical STM image obtained after deposition of 2HTTBPP on a Cu(110)–(2×1)O surface at a medium coverage at RT is shown in Figure 6a. Individual molecules and small ordered islands are simultaneously observed. The additional stripy features, mainly along the fast scanning direction, can be identified as diffusing molecules (much faster than the STM scanning speed) in a 2D gas phase that coexists with the 2D islands.[20,54] The existence of the 2D gas phase was also verified by using time-lapse STM movies, which show attaching and detaching molecules at the island borders (see Movie M1 in the Supporting Information).

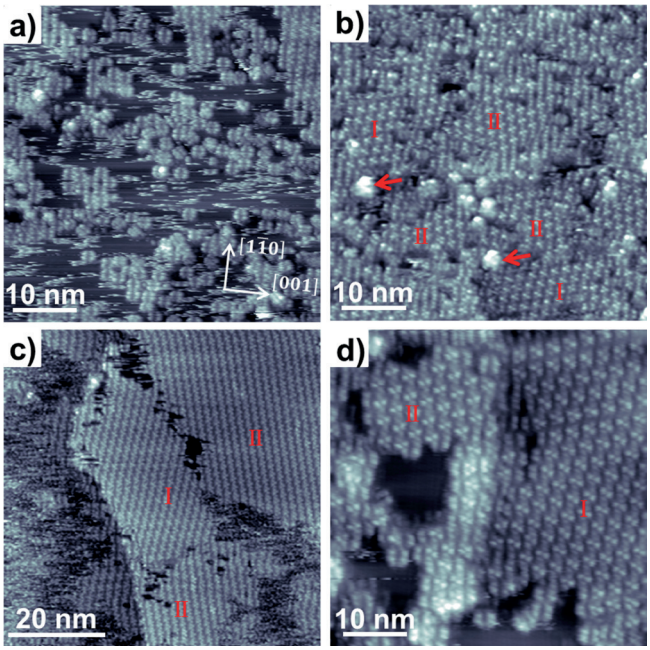

Figure 6. a, b) Constant-current STM images of medium and high coverage of 2HTTBPP on a Cu(110)–(2×1)O surface with deposition and measurement at RT, respectively. Note that the 2HTTBPP molecules self-metalate directly after deposition with the substrate copper atoms and form CuTTBPP molecules. c, d) Constant-current STM images of CuTTBPP on a Cu(110)–(2×1)O surface with deposition and measurement at RT. Tunneling parameters: a) $U=1.1$ V, $I=28$ pA; b) $U=-1.1$ V, $I=25$ pA; c) $U=-1.1$ V, $I=30$ pA; d) $U=-1.1$ V, $I=30$ pA.

By increasing the coverage to about one monolayer (Figure 6b), two apparently different types of domain coexist (labeled I and II), which are separated by disordered regions. In addition, bright dots (indicated by arrows; Figure 6b) are occasionally observed, which are attributed to molecules in the second layer.[20] The observation of highly mobile molecules in the 2D gas phase and the existence of a self-assembled supramolecular structure (which relies on the mobility of the building blocks) indicates that the strong molecule–substrate interaction and site specificity of the porphyrin molecules is at least significantly decreased by the presence of the (2×1)O reconstruction.[22,34] As a consequence, the formation of a supramolecular-ordered structure, in which the overall attractive molecule–molecule interaction dominates the adsorption behavior, is observed.[40,55]

It is important to note that Ballav and co-workers demonstrated that a reconstruction of Cu(100) surfaces by oxygen atoms significantly facilitates the self-metalation of 2HTPP at RT.[22] Thus, it could be anticipated that metalation also occurs in the present study upon deposition of 2HTTBPP on a Cu(110)–(2×1)O surface. Therefore, we also investigated the adsorption behavior of CuTTBPP on a Cu(110)–(2×1)O surface for comparison. Figure 6c,d depicts the STM images of a medium coverage of CuTTBPP on a Cu(110)–(2×1)O surface with deposition and measurement both at RT. Obviously, the appearance of CuTTBPP and 2HTTBPP after deposition at RT is identical, that is, the adsorbed species have the same intramolecular conformation and also self-assemble into the same supramolecular structure. The only difference is the size of the ordered domains, which are smaller for CuTTBPP formed by self-metalation (Figure 6b) relative to the directly deposited CuTTBPP (Figure 6d). Interestingly, the appearances of 2HTTBPP and CuTTBPP on the Cu(110)–(2×1)O surface after deposition at 180 K and measurement at 200 K are quite different (see Figure S4 in the Supporting Information). These observations strongly suggest that self-metalation of 2HTTBPP also occurs on the Cu(110)–(2×1)O surface between 200 K and RT and that the molecules imaged in Figure 6a,b are CuTTBPP formed by metalation of the deposited 2HTTBPP with copper substrate atoms.

The self-metalation mechanism of 2HTTBPP on Cu(110) and Cu(110)–(2×1)O surfaces at RT can be anticipated to be considerably different (discussed below). On a bare Cu(110) surface, the 2HTTBPP molecules react with copper atoms from the substrate to form CuTTBPP and gaseous dihydrogen: 2HTTBPP + Cu → CuTTBPP + H_2.[22,56] Previous gas-phase DFT studies of this reaction mechanism predict that iron and cobalt species react with porphyrin at RT, whereas elevated temperatures are required for copper and zinc atoms, as confirmed in various experimental studies.[19,42,51,56,57] As mentioned above, the self-metalation of 2HTTBPP on a Cu(110) surface at RT should be

accelerated by the comparably high copper-adatom density on the surface.[46,48] Recently, it was shown for 2HTPP on a Cu(111) surface by means of temperature-programmed desorption that the hydrogen atoms are not directly released as H_2 into the gas phase, but are transferred to the substrate and associatively desorb from there.[58] A similar mechanism is also likely to occur in our studies.

In contrast, different scenarios can be anticipated on the Cu(110)–(2×1)O surface. In the first scenario, the metalation process is accompanied by the release of one H_2O molecule per metalated porphyrin molecule (one oxygen atom from the oxygen reconstruction and two hydrogen atoms from 2HTTBPP): $2HTTBPP + CuO \rightarrow CuTTBPP + H_2O$.[22] Thereby, an intermediate state with Cu–O in the porphyrin species could be involved, thus facilitating the subsequent transfer of the hydrogen atoms to the oxygen atom and the formation of H_2O and CuTTBPP at RT.[56] A similar reaction mechanism has been proposed for the self-metalation of 2HTPP on an oxygen-covered Cu(001) surface.[22] The second scenario would be the formation of two OH groups on the surface, thus involving the oxygen atoms of the reconstructed substrate. Both scenarios could explain the formation of the smaller 2D islands for CuTTBPP generated through self-metalation as depicted in Figure 6b. In the course of the metalation process, both the consumption of the oxygen atoms during the water formation and, alternatively, the formation of two OH groups yield "defect states" on the surface, which could significantly change the surface corrugation such that diffusion is hindered or molecules are directly pinned due to their higher reactivity, that is, stronger chemical bonding.[39,59] In the latter case, these immobile molecules act as "blockers", thus effectively hindering the formation of large-area supramolecular structures.

To shed further light on the nature of the observed long-range-ordered supramolecular structures, high-resolution STM micrographs of individual CuTTBPP molecules were acquired and analyzed. Figure 7 depicts the overview of the two domain types along with high-resolution micrographs of the corresponding individual molecules (the two different domains and the corresponding intramolecular conformations are chiral; see the discussion below). The extracted intramolecular conformations are also shown. All the molecules in a specific domain have identical orientations. The lattice vectors of the unit cells are $a = 1.84 \pm 0.04$ and $b = 1.87 \pm 0.05$ nm, with an enclosed angle $\gamma = 117 \pm 5^\circ$, thus reflecting a hexagonal order within the margins of error (Figure 7a, b, e, f).

The high-resolution STM images (Figure 7c, g) reveal that each molecule exhibits eight protrusions, which correspond to the eight *tert*-butyl groups in each molecule. In addition, the four protrusions related to the upper *tert*-butyl groups show a different brightness, thus indicating different twist angles θ of the tBP groups within one molecule. From the side lengths of the formed rectangle of $l = 1.31 \pm 0.08$ and $s = 0.71 \pm 0.05$ nm (Figure 7d, h; see the Supporting Information for further details), the intramolecular conformation is deduced, thus yielding $\theta = 20 \pm 5$ and $10 \pm 5^\circ$ (for the two tBP groups, displayed in orange and yellow in Figure 6b, d, f, g, respectively) and $\varphi = 30 \pm 5^\circ$.

From the molecular arrangement shown in Figure 7b, f, we propose that the supramolecular structures are stabilized by attractive van der Waals interactions between the tBP groups

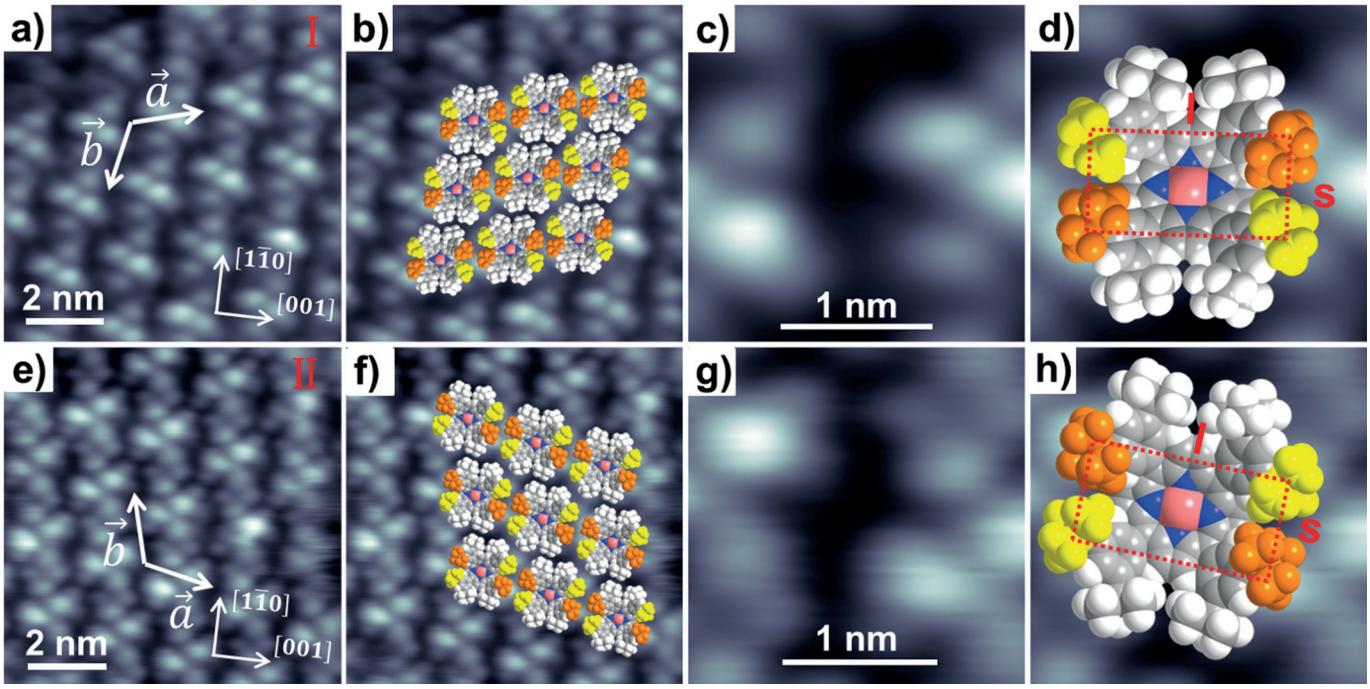

Figure 7. Overview of the observed two supramolecular porphyrin phases and the derived molecular models for CuTTBPP on a Cu(110)–(2×1)O surface. a–d) Structure I, e–h) structure II. Note that the 2HTTBPP molecules self-metalate directly after deposition with the substrate copper atoms to form CuTTBPP molecules. In the model, the four upper *tert*-butyl groups are depicted in yellow or orange due to different twist angles of the tBP groups. Tunneling parameters: a–d) $U = +1.1$ V, $I = 25$ pA; e–h) $U = +1.1$ V, $I = 30$ pA.

of neighboring molecules.[6,34,39] Intriguingly, all the *tert*-butyl groups in one molecule are arranged in a way that they are positioned close between two tBP substituents of neighboring molecules. This peculiar molecular arrangement might enhance attractive interactions between the corresponding side groups. A similar supramolecular structure with a similar intramolecular conformation (i.e., two different twist angles per molecule) has been observed previously for 2HTTBPP on a Cu(111) surface by Stark et al.[34]

Figure 8 shows a schematic illustration of the orientations of the unit cell and individual molecules in respect to the substrate for CuTTBPP on a Cu(110)–(2×1)O surface. For clarity,

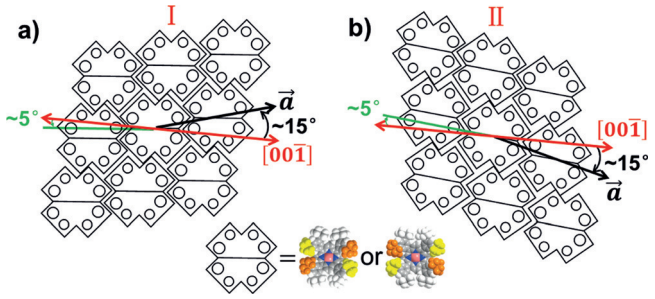

Figure 8. Schematic illustrations of the two molecular arrangements and orientations relative to the substrate for CuTTBPP on a Cu(110)–(2×1)O surface. The green lines point along the molecular axis of CuTTBPP. The black arrows indicate the unit cell vector $\vec{a}$. The models are scaled and positioned according to the arrangement extracted from the STM data in Figure 7.

the molecular axes (i.e., the connection between opposing pyrrole rings) are drawn as lines through the molecule. The unit cell vectors $\vec{a}$ (denoted as black arrows) are rotated by +15 or −15° (structures I and II, respectively) with respect to the [00$\bar{1}$] high symmetry direction of the Cu(110) surface (red arrows). In addition, the molecular axes (green lines) exhibit azimuthal angles of +5 and −5° in structures I and II, respectively, with respect to the substrate [00$\bar{1}$] direction. As a consequence, the two supramolecular structures are mirror images of each other, with the mirror plane perpendicular to the surface along the [001] direction of the Cu(110) surfaces. This behavior is referred to as organizational chirality, which has been reported previously for other porphyrin derivatives on metal surfaces and reconstructed metal surfaces.[20,28,39,60,61] A remarkable observation in the present case is that the individual molecules also exhibit chirality due to the specific intramolecular conformation. Overall, the adsorption behavior of CuTTBPP on the Cu(110)–(2×1)O surface can be thus regarded as another example of a chiral supramolecular structure formed by nonchiral molecules on a nonchiral surface.

Conclusions

We have reported the peculiar adsorption behavior of 2HTTBPP and CuTTBPP on pristine Cu(110) surfaces and the corresponding (2×1) reconstruction by oxygen atoms. CuTTBPP and 2HTTBPP adsorb in different intramolecular conformations at 200 K, mainly as individual molecules without the tendency to form supramolecular aggregates, diffuse, or rotate. Upon increasing the sample temperature to RT, the appearance of both molecular species is considerably modified to the same intramolecular conformation, that is, a flat conformation with the macrocycle and peripheral phenyl rings parallel to the surface. This observation was assigned to the thermally induced self-metalation of 2HTTBPP with copper atoms from the substrate and to an activated conformational change of both species; furthermore, temperatures higher than 200 K are required for both species to thermally overcome steric constrains in between the *ortho* substituents of the TTBPP species. The remarkable observation that CuTTBPP remains immobile even at RT was attributed to strong attractive molecule–substrate interactions. It was further demonstrated that the (2×1) surface reconstruction of Cu(110) by oxygen atoms significantly modifies the molecule–substrate interaction and facilitates the self-assembly of 2HTTBPP molecules at RT. As a result, the molecules arrange into supramolecular domains with two different 2D chiralities; interestingly, the individual molecules in these domains also reflect the different chirality through a specific intramolecular deformation. The self-assembly process is driven by a delicate balance between the molecule–molecule and molecule–substrate interactions. Notably, 2HTTBPP self-metalates to CuTTBPP at RT and on the Cu(110)–(2×1)O surface. Our results indicate that reconstruction on metal surfaces can greatly modify molecule–substrate interactions, which should be a promising route to engineer functional porphyrin nanoarchitectures.

Experimental Section

The sample preparation and STM experiments were performed in a two-chamber UHV system with a base pressure in the range of 10^{-10} mbar. The microscope used was an RHK UHV VT STM 300 with RHK SPM 100 electronics. The STM images were acquired at room temperature (RT) or 200 K in the constant-current mode with a Pt/Ir tip. The given bias voltages refer to the sample. The STM images were processed by using WSxM software.[62] Background subtraction and moderate filtering (Gaussian smooth) were applied to the STM images. Cu(110) single crystals were prepared by repeated cycles of Ar^+ sputtering (500 eV) and annealing to 850 K. The Cu(110)–(2×1)O surface was prepared by dosing with O_2 (600 Langmuir, 1 L = 1.3×10^{-6} mbar s; purity = 99.99%), whilst keeping the sample temperature at 500 K. The introduction of O_2 was realized by backfilling the chamber through a leak valve. The 2HTTBPP and CuTTBPP molecules were deposited onto the substrates at RT or 180 K by thermal sublimation from a home-built Knudsen cell at 620 K.

Acknowledgements

The authors gratefully acknowledge the funding by the German Research Council (DFG) through research unit FOR 1878/funCOS, the Cluster of Excellence "Engineering of Advanced Materials" (http://www.eam.uni-erlangen.de), and the Collaborative Research Center SFB 953 at the Friedrich-Alexander-Universität Erlangen-Nürnberg. L.Z. thanks the Alexander von Humboldt Foundation for a research fellowship.

Keywords: adsorption · porphyrinoids · scanning tunneling microscopy · self-assembly · surfaces and interfaces

[1] J. V. Barth, G. Costantini, K. Kern, *Nature* **2005**, *437*, 671 – 679.
[2] F. Klappenberger, *Prog. Surf. Sci.* **2014**, *89*, 1 – 55.
[3] W. Auwärter, D. Écija, F. Klappenberger, J. V. Barth, *Nat. Chem.* **2015**, *7*, 105 – 120.
[4] L. Bartels, *Nat. Chem.* **2010**, *2*, 87 – 95.
[5] H. Marbach, H.-P. Steinrück, *Chem. Commun.* **2014**, *50*, 9034.
[6] S. Ditze, M. Stark, F. Buchner, A. Aichert, N. Jux, N. Luckas, A. Görling, W. Hieringer, J. Hornegger, H.-P. Steinrück, H. Marbach, *J. Am. Chem. Soc.* **2014**, *136*, 1609 – 1616.
[7] S. Ditze, M. Stark, M. Drost, F. Buchner, H.-P. Steinrück, H. Marbach, *Angew. Chem. Int. Ed.* **2012**, *51*, 10898 – 10901.
[8] J. Otsuki, *Coord. Chem. Rev.* **2010**, *254*, 2311 – 2341.
[9] J. M. Gottfried, *Surf. Sci. Rep.* **2015**, *70*, 259 – 379.
[10] H. Marbach, *Acc. Chem. Res.* **2015**, *48*, 2649 – 2658.
[11] J. K. Gimzewski, C. Joachim, *Science* **1999**, *283*, 1683 – 1688.
[12] T. A. Jung, R. R. Schlittler, J. K. Gimzewski, *Nature* **1997**, *386*, 696 – 698.
[13] F. Buchner, E. Zillner, M. Röckert, S. Gläßel, H.-P. Steinrück, H. Marbach, *Chem. Eur. J.* **2011**, *17*, 10226 – 10229.
[14] M. Stark, S. Ditze, M. Drost, F. Buchner, H.-P. Steinrück, H. Marbach, *Langmuir* **2013**, *29*, 4104 – 4110.
[15] M. In't Veld, P. Iavicoli, S. Haq, D. B. Amabilino, R. Raval, *Chem. Commun.* **2008**, 1536 – 1538.
[16] F. Buchner, K. Comanici, N. Jux, H.-P. Steinrück, H. Marbach, *J. Phys. Chem. C* **2007**, *111*, 13531 – 13538.
[17] L. Grill, M. Dyer, L. Lafferentz, M. Persson, M. V. Peters, S. Hecht, *Nat. Nanotechnol.* **2007**, *2*, 687 – 691.
[18] F. Buchner, J. Xiao, E. Zillner, M. Chen, M. Röckert, S. Ditze, M. Stark, H.-P. Steinrück, J. M. Gottfried, H. Marbach, *J. Phys. Chem. C* **2011**, *115*, 24172 – 24177.
[19] K. Diller, F. Klappenberger, M. Marschall, K. Hermann, A. Nefedov, C. Wöll, J. V. Barth, *J. Chem. Phys.* **2012**, *136*, 014705.
[20] F. Buchner, I. Kellner, W. Hieringer, A. Görling, H.-P. Steinrück, H. Marbach, *Phys. Chem. Chem. Phys.* **2010**, *12*, 13082 – 13090.
[21] D. Chylarecka, C. Wackerlin, T. K. Kim, K. Müller, F. Nolting, A. Kleibert, N. Ballav, T. A. Jung, *J. Phys. Chem. Lett.* **2010**, *1*, 1408 – 1413.
[22] J. Nowakowski, C. Wäckerlin, J. Girovsky, D. Siewert, T. A. Jung, N. Ballav, *Chem. Commun.* **2013**, *49*, 2347.
[23] S. Ditze, M. Röckert, F. Buchner, E. Zillner, M. Stark, H.-P. Steinrück, H. Marbach, *Nanotechnology* **2013**, *24*, 115305.
[24] T. Suzuki, T. Lutz, D. Payer, N. Lin, S. L. Tait, G. Costantini, K. Kern, *Phys. Chem. Chem. Phys.* **2009**, *11*, 6498 – 6504.
[25] M. El Garah, J. Lipton-Duffin, J. M. MacLeod, R. Gutzler, F. Palmino, V. Luzet, F. Cherioux, F. Rosei, *Chem. Asian J.* **2013**, *8*, 1813 – 1817.
[26] M. Oehzelt, L. Grill, S. Berkebile, G. Koller, F. P. Netzer, M. G. Ramsey, *Chemphyschem* **2007**, *8*, 1707 – 1712.
[27] M. Oehzelt, S. Berkebile, G. Koller, J. Ivanco, S. Surnev, M. G. Ramsey, *Surf. Sci.* **2009**, *603*, 412 – 418.
[28] M. Wagner, P. Puschnig, S. Berkebile, F. P. Netzer, M. G. Ramsey, *Phys. Chem. Chem. Phys.* **2013**, *15*, 4691 – 4698.
[29] L. Smykalla, P. Shukrynau, D. R. T. Zahn, M. Hietschold, *J. Phys. Chem. A* **2015**, *119*, 17228 – 17234.
[30] T. Yokoyama, Y. Tomita, *J. Chem. Phys.* **2008**, *129*, 164704.
[31] Y. Kuk, F. Chua, P. Silverman, J. Meyer, *Phys. Rev. B* **1990**, *41*, 12393.
[32] H. Dürr, R. Schneider, T. Fauster, *Phys. Rev. B* **1991**, *43*, 1802.
[33] Z. X. Wang, F. H. Tian, *J. Phys. Chem. B* **2003**, *107*, 6153 – 6161.
[34] M. Stark, S. Ditze, M. Lepper, L. Zhang, H. Schlott, F. Buchner, M. Röckert, M. Chen, O. Lytken, H.-P. Steinrück, *Chem. Commun.* **2014**, *50*, 10225 – 10228.
[35] T. Yokoyama, S. Yokoyama, T. Kamikado, Y. Okuno, S. Mashiko, *Nature* **2001**, *413*, 619 – 621.
[36] T. Yokoyama, Y. Tomita, *J. Chem. Phys.* **2012**, *137*, 244701.
[37] T. Wölfle, A. Görling, W. Hieringer, *Phys. Chem. Chem. Phys.* **2008**, *10*, 5739 – 5742.
[38] T. Jung, R. Schlittler, J. Gimzewski, H. Tang, C. Joachim, *Science* **1996**, *271-274*, 181 – 183.
[39] L. Zhang, M. Lepper, M. Stark, D. Lungerich, N. Jux, W. Hieringer, H.-P. Steinrück, H. Marbach, *Phys. Chem. Chem. Phys.* **2015**, *17*, 13066 – 13073.
[40] J. Xiao, S. Ditze, M. Chen, F. Buchner, M. Stark, M. Drost, H.-P. Steinrück, J. M. Gottfried, H. Marbach, *J. Phys. Chem. C* **2012**, *116*, 12275 – 12282.
[41] M. Röckert, M. Franke, Q. Tariq, S. Ditze, M. Stark, P. Uffinger, D. Wechsler, U. Singh, J. Xiao, H. Marbach, H.-P. Steinrück, O. Lytken, *Chem. Eur. J.* **2014**, *20*, 8948 – 8953.
[42] K. Diller, F. Klappenberger, F. Allegretti, A. C. Papageorgiou, S. Fischer, A. Wiengarten, S. Joshi, K. Seufert, D. Écija, W. Auwärter, J. V. Barth, *J. Chem. Phys.* **2013**, *138*, 154710.
[43] G. Di Santo, S. Blankenburg, C. Castellarin-Cudia, M. Fanetti, P. Borghetti, L. Sangaletti, L. Floreano, A. Verdini, E. Magnano, F. Bondino, C. A. Pignedoli, M. T. Nguyen, R. Gaspari, D. Passerone, A. Goldoni, *Chem. Eur. J.* **2011**, *17*, 14354 – 14359.
[44] K. Comanici, F. Buchner, K. Flechtner, T. Lukasczyk, J. M. Gottfried, H.-P. Steinrück, H. Marbach, *Langmuir* **2008**, *24*, 1897 – 1901.
[45] W. Auwärter, A. Weber-Bargioni, S. Brink, A. Riemann, A. Schiffrin, M. Ruben, J. V. Barth, *Chemphyschem* **2007**, *8*, 250 – 254.
[46] A. Goldoni, C. A. Pignedoli, G. Di Santo, C. Castellarin-Cudia, E. Magnano, F. Bondino, A. Verdini, D. Passerone, *ACS Nano* **2012**, *6*, 10800 – 10807.
[47] R. González-Moreno, A. Garcia-Lekue, A. Arnau, M. Trelka, J. M. Gallego, R. Otero, A. Verdini, C. Sánchez-Sánchez, P. L. de Andrés, J. Á. Martín-Gago, C. Rogero, *J. Phys. Chem. C* **2013**, *117*, 7661 – 7668.
[48] R. González-Moreno, C. Sánchez-Sánchez, M. Trelka, R. Otero, A. Cossaro, A. Verdini, L. Floreano, M. Ruiz-Bermejo, A. García-Lekue, J. A. n. Martín-Gago, C. Rogero, *J. Phys. Chem. C* **2011**, *115*, 6849 – 6854.
[49] C. Perry, S. Haq, B. Frederick, N. Richardson, *Surf. Sci.* **1998**, *409*, 512 – 520.
[50] W. Auwärter, F. Klappenberger, A. Weber-Bargioni, A. Schiffrin, T. Strunskus, C. Wöll, Y. Pennec, A. Riemann, J. V. Barth, *J. Am. Chem. Soc.* **2007**, *129*, 11279 – 11285.
[51] F. Klappenberger, A. Weber-Bargioni, W. Auwärter, M. Marschall, A. Schiffrin, J. V. Barth, *J. Chem. Phys.* **2008**, *129*, 214702.
[52] R. Otero, F. Hummelink, F. Sato, S. B. Legoas, P. Thostrup, E. Laegsgaard, I. Stensgaard, D. S. Galvao, F. Besenbacher, *Nat. Mater.* **2004**, *3*, 779 – 782.
[53] Q. Sun, C. Zhang, Z. Li, K. Sheng, H. Kong, L. Wang, Y. Pan, Q. Tan, A. Hu, W. Xu, *Appl. Phys. Lett.* **2013**, *103*, 013103.
[54] D. E. Barlow, L. Scudiero, K. Hipps, *Langmuir* **2004**, *20*, 4413 – 4421.
[55] M. Röckert, S. Ditze, M. Stark, J. Xiao, H.-P. Steinrück, H. Marbach, O. Lytken, *J. Phys. Chem. C* **2013**, *117*, 1661 – 1667.
[56] T. E. Shubina, H. Marbach, K. Flechtner, A. Kretschmann, N. Jux, F. Buchner, H.-P. Steinrück, T. Clark, J. M. Gottfried, *J. Am. Chem. Soc.* **2007**, *129*, 9476 – 9483.
[57] J. M. Gottfried, K. Flechtner, A. Kretschmann, T. Lukasczyk, H.-P. Steinrück, *J. Am. Chem. Soc.* **2006**, *128*, 5644 – 5645.
[58] M. Röckert, M. Franke, Q. Tariq, D. Lungerich, N. Jux, M. Stark, A. Kaftan, S. Ditze, H. Marbach, M. Laurin, J. Libuda, H.-P. Steinrück, O. Lytken, *J. Phys. Chem. C* **2014**, *118*, 26729 – 26736.
[59] P. Rahe, M. Nimmrich, A. Nefedov, M. Naboka, C. Woll, A. Kuhnle, *J. Phys. Chem. C* **2009**, *113*, 17471 – 17478.
[60] W. Auwärter, A. Weber-Bargioni, A. Riemann, A. Schiffrin, O. Gröning, R. Fasel, J. V. Barth, *J. Chem. Phys.* **2006**, *124*, 194708.
[61] K.-H. Ernst, *Phys. Status Solidi B* **2012**, *249*, 2057 – 2088.
[62] I. Horcas, R. Fernández, J. M. Gómez-Rodríguez, J. Colchero, J. Gómez-Herrero, A. M. Baro, *Rev. Sci. Instrum.* **2007**, *78*, 013705.

Received: October 19, 2015
Published online on February 2, 2016